Trapped planar three-boson system with spin 1 and with hard-core interactions

C. G. Bao and T. Y. Shi
State Key Laboratory of Optoelectronic Materials and Technologies, and Department of Physics, Zhongshan University, Guangzhou 510275, People's Republic of China
(Received 25 May 2003; published 24 September 2003)

A two-dimensional spin 1 three-boson system trapped by a parabolic confinement and interacting with hard-core repulsion has been investigated. The spectrum has been analyzed in detail, in particular, the existence of breathing bands has been confirmed. Two density functions associated with the oscillations of breathing and deformation, respectively, have been defined to study the structure of low-lying states. The inherent nodal structure of wave functions is found to play a decisive role. The effect of rotation on the ground-state property has also been studied. Not only the angular momentum, the permutation symmetry will also transit in accord with the increase of the speed of rotation.

DOI: 10.1103/PhysRevA.68.032509 PACS number(s): 36.10.−k

I. INTRODUCTION

The achievement of Bose-Einstein condensates (BECs) in trapped atomic gas has stimulated explosively growing interest in the systems of interacting bosons [1,2]. In recent years, much attention has been devoted to BECs in lower dimensions. It is expected that the character and spectrum of the collective excitation of the BECs in lower dimensions would exhibit a qualitative change compared to their three-dimensional counterpart. More stable topological excitations such as solitons (in one dimension) and vortices (in two dimension) would be achieved [3,4]. The experimental realization of BEC in quasi-two-dimension and in quasi-one-dimension has been reported by several groups [5–8]. Theoretical studies for interacting bosons in two dimension are mainly focused on the rotating properties and the vortex structures of systems in the Thomas-Fermi limit of strong interactions [9–11] as well as in the limit of weak interactions [12–20]. The former limit case is closely related to the current experiments. Moreover, in this limit case the predictions of the mean-field theory take a rather simple analytic form. The latter limit case is also of great theoretical interest due to the mesoscopic nature of system, originating from the fact that the coherence length in the atomic cloud becomes larger than the size of the system, and also due to the available analytic solution of many-body wave functions, which is analagous to the well-known Laughlin wave functions in the quantum Hall regime in two-dimensional electron gas [21–24]. Also, in this limit exact diagonalization method for few boson systems is performed in the framework of lowest Landau level approximation. Besides, the ground-state properties in the transition regime of middle interaction are also discussed by several authors [25,26].

While the ground-state properties of the interacting boson systems have been studied extensively, the low-lying excited states have also attracted a lot of attention due to their crucial roles in determining the thermodynamic behavior of the systems and in understanding the stability of the ground states under external perturbations [13,17,20]. It is shown that the low-lying excited states in the case of weak-interaction limit are dominant by the collective multipole excitation associated with the multipole deformations of systems. However, for the higher-lying states, there is monopole excitation (or breathing mode which is associated with the collective radial excitation) in the two-dimensional Bose systems with contact interaction. Pitaevskii and Rosch have pointed out that a two-dimensional harmonically trapped Bose system with contact interaction displays breathing modes, and that the corresponding states have energies that differ by exactly two oscillator spacings [27]. This property, which is independent of the strength of interaction, can be related to the existence of a hidden symmetry of the problem described by two-dimensional Lorentz group SO(2,1). The breathing modes in the case of none-contact interaction are also discussed by Bao *et al.* [28]. Very recently, such a breathing mode has been observed experimentally [29].

In this paper, we would extend our study on three spin 0 bosonic system [28] to the case that bosons have internal degree of freedom, hyperfine spin. The study of such a three-boson system with internal degree of freedom is important for several reasons. First, the energy spectrum of such a few-body system can be obtained by exact diagonalization method. The correlation between particles which is discarded in mean-field approximation can be fully taken into account. Second, the recent experimental observation of quantum phase transition from a superfluid to a Mott insulator in a gas of ultracold atoms provide a novel possibility for exploring the properties of few-body systems [30]. In the experiment described in Ref. [30] up to 200 000 ^{87}Rb atoms were distributed over more than 15 000 lattice sites, thereby creating a large number of few-body system with up to 2.5 atoms each on average. Third, the spinor BEC is also an active field in BEC physics [31–35]. The introduction of internal degree of freedom would enrich physics. Our main interest in this paper is the whole energy spectrum structure of three spin-1 boson system, especially the band structure of the breathing mode. Emphasis is placed on the study of symmetry effects.

II. SPIN STATES, HAMILTONIAN, AND DIAGONALIZATION

Let three identical bosons be trapped in a plane by a parabolic confinement with a strength $\hbar\omega_0$. Each boson has a mass m and a spin equal to 1. We use $\hbar\omega_0$ and $\sqrt{\hbar/m\omega_0}$ as

units of energy and length, respectively, throughout the paper. It is assumed, as in our previous paper on a three-boson system with spin 0 [28], that the bosons interact with each other via a spin-independent hard-core repulsive potential $U\Theta(b-r_{ij})$, where U and b are positive constants, r_{ij} is the interparticle distance, and $\Theta(x)=1$ if $x\geqslant 0$ or $\Theta(x)=0$ if $x<0$. Let $\mathbf{r}_i$ be the position vector of the ith boson. A set of Jacobi coordinates $\mathbf{r}$ and R is adopted, $\mathbf{r}=\mathbf{r}_2-\mathbf{r}_1$ and $\mathbf{R}=\mathbf{r}_3-\frac{1}{2}(\mathbf{r}_1+\mathbf{r}_2)$. In the center-of-mass frame the internal Hamiltonian reads

$$H_I=-\nabla_r^2+\frac{1}{4}r^2-\frac{3}{4}\nabla_R^2+\frac{1}{3}R^2+\sum_{i<j}U\Theta(b-r_{ij}). \quad (1)$$

In order to diagonalize H_I, let us first introduce a virtual adjustable single-particle Hamiltonian of harmonic oscillation $-(1/2\mu)\nabla_s^2+\frac{1}{2}\mu v^2 s^2$. Here, $\vec{s}$ is a two-dimensional vector, μ is related to the reduced mass, and v is an adjustable parameter. Let $\varphi_{mk}(\sqrt{\mu v}\vec{s})$ be an eigenstate of this harmonic oscillation with an eigenenergy $(m+k+1)v$ and an angular momentum $(m-k)$. These single-particle states will be used to compose the basis functions to expand the eigenstates of H_I.

Let a spin state of a single boson be denoted as χ and a spin state of the three-boson system be denoted as

$$|s,S\rangle=[(\chi(1)\chi(2))_s\chi(3)]_S, \quad (2)$$

where the spins of the particles 1 and 2 are coupled to s, then s and the spin of the third are coupled to the total spin S. In what follows $|s,S\rangle$ are combined to form the basis states $\eta_S^{\lambda,i}$ of the representation λ of the permutation group, $\lambda=\{3\},\{2,1\}$, or $\{1,1,1\}$. $\eta_S^{\lambda,i}$ are related to $|s,S\rangle$ as follows [36].

(i) When $S=3$, the spin state $|2,3\rangle$ belongs to the one-dimensional representation $\lambda=\{3\}$, we have

$$\eta_3^{\{3\},1}=|2,3\rangle.$$

(ii) When $S=2$, $\lambda=\{2,1\}$, we have

$$\eta_2^{\{2,1\},1}=|1,2\rangle \quad \text{and} \quad \eta_2^{\{2,1\},2}=|2,2\rangle.$$

(iii) When $S=1$, the three spin-states $|0,1\rangle$, $|1,1\rangle$, and $|2,1\rangle$ belong to two representations $\lambda=\{3\}$ and $\{2,1\}$, we have

$$\eta_1^{\{3\},1}=\frac{\sqrt{5}}{3}|0,1\rangle+\frac{2}{3}|2,1\rangle,$$

$$\eta_1^{\{2,1\},1}=|1,1\rangle,$$

$$\eta_1^{\{2,1\},2}=\frac{2}{3}|0,1\rangle-\frac{\sqrt{5}}{3}|2,1\rangle.$$

(iv) When $S=0$, $\lambda=\{1,1,1\}$, we have

$$\eta_0^{\{1,1,1\},1}=|1,0\rangle.$$

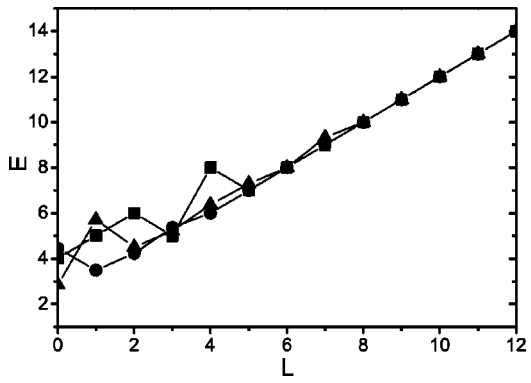

FIG. 1. The energies $E_i^{L,\lambda}$ of the first states, where the triangle is for $\lambda=\{3\}$, the circle for $\lambda=\{2,1\}$, and the square for $\lambda=\{1,1,1\}$.

Now a totally symmetric eigenstate of H_I with a given angular momentum L, a spatial permutation symmetry λ, and a total spin S can be expanded as

$$\Psi_{L\lambda S}=\sum_i F_{L\lambda i}\,\eta_S^{\lambda,i}, \quad (3)$$

where $F_{L\lambda i}$ is a spatial function which can be expanded as

$$F_{L\lambda i}=\sum_Q C_Q P_{\lambda i}\left[\varphi_{mk}\left(\sqrt{\frac{v}{2}}\mathbf{r}\right)\varphi_{MK}\left(\sqrt{\frac{2v}{3}}\mathbf{R}\right)\right]. \quad (4)$$

Here, Q denotes the set $(mkMK)$, $\mathbf{P}_{\lambda i}$ is the projection operator onto the space of representation λ, $m-k+M-K=L$ is assumed, and v serves as a variational parameter. With this expansion the Schrödinger equation can be written in a matrix form and the matrix elements can be calculated. The eigenstates $\Psi_{L\lambda S}$ and the eigenenergies can be obtained after the diagonalization of H_I. It turns out that, when v is given at its optimal value, less than 2000 independent basis functions included in the expansion are sufficient to provide solutions accurate enough for our purpose.

III. SPECTRUM

As in the Ref. [28], let us first make the choice that $U=200$ and $b=0.1$. The other choices of parameters will be discussed later. Since the Hamiltonian is spin independent, the eigenenergies do not depend directly on S, but depend on L and λ. It is noted that when $\lambda=\{3\}$, S can be equal to 3 or 1. Thus the levels are degenerate with respect to S. When $\lambda=\{2,1\}$, S can be equal to 2 or 1. However, when $\lambda=\{1,1,1\}$, S can be only equal to zero. Incidentally, there is also a degeneracy with respect to the interchange of L and $-L$. In what follows, it is sufficient to discuss only the $L\geqslant 0$ states.

The states having the same λ and L constitute a series. Let L_i^λ denotes the ith state of this series with an energy $E_i^{L,\lambda}$. The first state L_1^λ is the lowest of the series. The energies $E_1^{L,\lambda}$ of the first states are plotted in Fig. 1. To explain the spectrum we have to mention the following points.

(i) If the hard-core repulsion is removed, the three bosons would all stay in the lowest harmonic oscillation levels,

TABLE I. The number of favorable basis functions allowed in a state with given L and λ.

L	0	1	2	3	4	5	6	7	$\geqslant 8$
$\{3\}$	1	0	1	1	1	1	2	1	$\geqslant 2$
$\{2,1\}$	0	1	1	1	2	2	2	3	$\geqslant 3$
$\{1,1,1\}$	0	0	0	1	0	1	1	1	$\geqslant 1$

namely, the levels having $k=K=0$. However, due to the effect of the permutation symmetry, these favorable basis functions might not be allowed for a state with specified λ and L. The number of the allowed favorable basis functions can be easily evaluated from the basics of group theory as shown in Table I.

For example, if $\lambda=\{2,1\}$ and when $L=6$ the number of favorable basis functions is 2, and when $L\geqslant 8$ the number is $\geqslant 3$.

Obviously, once the favorable basis functions are prohibited, the prohibition will lead to an increase in energy. For example, for $L=0$ states, favorable basis functions are allowed only in $\lambda=\{3\}$ states, thus $E_1^{0,\{3\}}$ should be remarkably lower than $E_1^{0,\{2,1\}}$ and $E_1^{0,\{111\}}$, just as shown in Fig. 1. Similarly, for $L=1$, $E_1^{1,\{2,1\}}$ should be lower than $E_1^{1,\{3\}}$ and $E_1^{1,\{111\}}$, for $L=2$, $E_1^{2,\{111\}}$ should be explicitly higher than the other two, and so on. When L is not large the number of favorable basis functions depends strongly on λ, therefore $E_1^{L,\lambda}$ depends also strongly on λ as shown in Fig. 1.

(ii) In the $\{1,1,1\}$ symmetry any particle is scarcely to be close to another particle because the wave function has to be zero if they overlap. Furthermore, the range of hard-core repulsion b is small. Thus, the probability of a pair of particles staying inside b is very small resulting in a very weak repulsion. For all the $\lambda=\{1,1,1\}$ states, due to the very weak repulsion, the energy levels are found to be very close to those of pure harmonic oscillation. In fact, the levels with $\lambda=\{1,1,1\}$ in Fig. 1 lie either very close to the straight lines $E_1^{L,\lambda}=L+2$ or $E_1^{L,\lambda}=L+4$.

(iii) It is shown in Table I that more than one favorable basis function (i.e., $k=K=0$) would be contained if L is larger, e.g., the $4_i^{\{2,1\}}$ states have two favorable basis functions. It was found that these basis functions can mixed up in such a way that one of the eigenstate can be nearly free from the hard-core repulsion. For example, $E_1^{4,\{2,1\}}$ and $E_2^{4,\{2,1\}}$ states are 6.003 and 6.304, respectively, the former is close to the pure harmonic oscillation energy 6. For another example, $E_1^{6,\{3\}}$ and $E_2^{6,\{3\}}$ states are 8.000 and 8.338, respectively, the former does not have hard-core repulsion. Since more than one favorable basis function is contained if L is larger, $E_1^{L,\lambda}$ will tend to $L+2$ disregarding λ, namely, tend to the energy of harmonic oscillation. This is the reason that the curves in Fig. 1 converge to a straight line. This feature is common to the systems with short-range repulsion. Incidentally, when L is larger, the level of the L_1^λ state is highly degenerate because it has four choices in S.

(iv) The last factor affecting energies is the nodal structure of wave functions. It is well known that if a wave function contains nodal surfaces, the kinetic energy would increase. The more nodal surfaces are contained, the higher the energy. Since a first-state L_1^λ is the lowest of a series, it would do its best to lower the energy. Therefore, it would contain nodal surfaces as least as possible. However, wave functions may contain inherently a kind of nodal surfaces imposed by symmetry [37–39], this is explained as follows.

When the three bosons turn out to form an equilateral triangle (ET), then a rotation about the c.m. by 120° is equivalent to a cyclic permutation of particles. Thus, we have

$$\exp\left(i\frac{2\pi}{3}L\right)F_{L\lambda i}(123)=F_{L\lambda i}(231)=P_cF_{L\lambda i}(123)$$

$$=\sum_j M_{ij}^\lambda(P_c)F_{L\lambda j}(123), \qquad (5)$$

where P_c is the operator of the cyclic permutation and $M_{ij}^\lambda(P_c)$ is the associated matrix element of the λ representation. It is emphasized that this equation holds only if the coordinates form an ET. Let us discuss in detail the more complicated case of $\lambda=\{2,1\}$. When $i=1$ and 2, using the knowledge of the theory of representation, the above equation can be rewritten, respectively, as

$$\exp\left(i\frac{2\pi}{3}L\right)F_{L\lambda 1}(\triangle)=-\frac{1}{2}F_{L\lambda 1}(\triangle)+\frac{\sqrt{3}}{2}F_{L\lambda 2}(\triangle), \qquad (6)$$

$$\exp\left(i\frac{2\pi}{3}L\right)F_{L\lambda 2}(\triangle)=-\frac{\sqrt{3}}{2}F_{L\lambda 1}(\triangle)-\frac{1}{2}F_{L\lambda 2}(\triangle), \qquad (7)$$

where $(\triangle)$ denotes that the coordinates form an ET. This is a set of homogeneous linear equations; the determinant of this set $\mathrm{Det}=2\cos[(2\pi/3)L]+1$. Evidently, this set would have a nonzero solution only if $\mathrm{Det}=0$ or $L\neq 3I$, here $I=0,1,2,\ldots$. It implies that both $F_{L\lambda i}$ would be zero at any ET if $L=3I$. In this case an inherent nodal surface emerges at the ETs, and this shape is therefore inaccessible to the $(L,\lambda)=(3I,\{2,1\})$ states.

When the three bosons turn out to form a cigar shape with two at the two ends and one at the middle (denoted as CG1), then a rotation about the c.m. by 180° is equivalent to an interchange of the pair of particles at the two ends. This equivalence leads also to a constraint and inherent nodal surfaces might also occur at the CG1. Therefore, the CG1 may also be inaccessible to certain states. The accessibility of shapes are listed in Table II.

It is recalled that the spectrum in Fig. 1 has been explained based on Table I. However, it can also be equivalently explained based on Table II. For this purpose, let H_I be exactly rewritten in a new form as

$$H_I=\mathbf{T}+\mathbf{U}, \qquad (8)$$

$$\mathbf{T}=-\nabla_r^2-\tfrac{3}{4}\nabla_R^2, \qquad (9)$$

TABLE II. The accessibility of regular shapes, where a block with an "*a*" implies that the shape is accessible to the associated state; e.g., the CG1 is accessible to the $\lambda=\{111\}$ and L odd states. A cross implies inaccessible.

		$L=$	0	1	2	3	4	5	6
{3}	ET		*a*	×	×	*a*	×	×	*a*
{3}	CG1		*a*	×	*a*	×	*a*	×	*a*
{2,1}	ET		×	*a*	*a*	×	*a*	*a*	×
{2,1}	CG1		*a*	*a*	*a*	*a*	*a*	*a*	*a*
{111}	ET		*a*	×	×	*a*	×	×	*a*
{111}	CG1		×	*a*	×	*a*	×	*a*	×

$$\mathbf{U}=\sum_{i<j}\left[\tfrac{1}{6}r_{ij}^2+U\Theta(b-r_{ij})\right]. \tag{10}$$

In this form the parabolic confinement is replaced by the quadratic terms in the pairwise interaction. From this form we see that the distance between any pair of particles should neither be too large nor too small. If it is too large, the quadratic term in **U** would cause a remarkable increase of energy. If it is too small, the hard core would cause also a great increase of energy. Thus, there is an optimal domain of separation between the particles. If the bosons form an ET, then the interparticle distances can be simultaneously optimized. Therefore this shape would be favorable to binding. Whereas only two distances can be simultaneously optimized if a CG1 is formed, thus the CG1 is not as favorable as the ET.

It is recalled that all the first states will do their best to lower the energy; for this purpose the distributions of wave function in coordinate space are optimized. However, the optimization will be affected by the accessibility of regular shapes. Therefore, it would be useful to classify the states according to their ability to get access to regular shapes. There are four types of states. The first type can get access to both the ET and CG1, the second can only get access to the ET but not the CG1, the third can only get access to the CG1 but not the ET, the fourth cannot get access to both the ET and CG1. Based on Table II, the types of states are listed in Table III.

Since the prohibition of shapes would affect the optimization of wave functions, in particular, the prohibition of favorable shapes would cause a severe effect, it is reasonable to assume that, for a given L, the energy of the first state of the first type is the lowest, the second type is the second lowest, while the fourth type is the highest. If this is true, the energies for the $L=0$ first states in ascending order would be $E_1^{0,\{3\}}$, $E_1^{0,\{111\}}$, and $E_1^{0,\{2,1\}}$ having the types I, II, and III, respectively, as shown in Table III, the energies for $L=1$ would be $E_1^{1,\{2,1\}}$, $E_1^{1,\{111\}}$, and $E_1^{1,\{3\}}$ having the types I, III, and IV, respectively. It turns out that these suggested sequences are just the same as in Fig. 1. In fact, for each of the L under consideration, the sequence according to the types is just the sequence from numerical calculation, no exception is found. E.g., the energies of $6_1^{\{3\}}$, $6_1^{\{111\}}$, and $6_1^{\{2,1\}}$ associated with the types I, II, and III are 8.0000, 8.0013, and 8.0029, respectively. Although these three levels are too close to each other to be distinguished in Fig. 1, they are still ordered exactly according to the types. Thus the effect of accessibility on the level ordering is undoubted and the classification is reasonable. Incidentally, the explanation based on Table III is better than the explanation based on Table I in explaining the details of the spectrum. For example, why $E_1^{2,\{2,1\}}$ is lower than $E_1^{2,\{3\}}$, why $E_1^{3,\{3\}}$ is lower than $E_1^{3,\{2,1\}}$, etc., can be explained now but not earlier.

IV. DENSITY FUNCTIONS

In order to understand the particle correlation, in what follows a detailed analysis of wave functions will be made. First, we introduce the hyperradius

$$\xi=\sqrt{\frac{1}{2}r^2+\frac{2}{3}R^2} \tag{11}$$

and a new argument

$$\beta=\frac{2}{3}\left(\frac{R}{\xi}\right)^2. \tag{12}$$

Here β is related to the usually defined hyperangle α by $\beta=\sin^2\alpha$. The domain of β is from 0 to 1, while α is from 0 to $\pi/2$. The correlated densities extracted below using β as argument is invariant under particle permutations; this is the

TABLE III. Four types of states.

	L	0	1	2	3	4	5	6
{3}		I	IV	III	II	III	IV	I
{2,1}		III	I	I	III	I	I	III
{111}		II	III	IV	I	IV	III	II

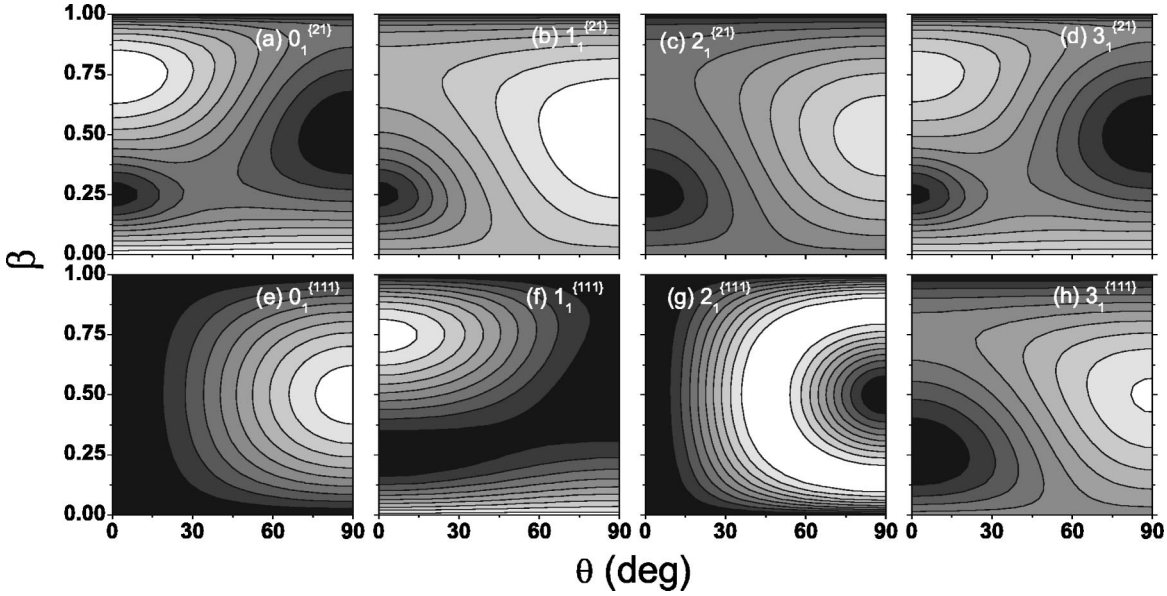

FIG. 2. $\rho(\theta,\beta)$ of the $L_1^{\{2,1\}}$ and $L_1^{\{111\}}$ first states. The darker area has a smaller $\rho(\theta,\beta)$.

reason why we use β to replace α. Let the azimuthal angles of $\mathbf{r}$ and $\mathbf{R}$ be ϕ_r and ϕ_R. The volume element can be written as

$$d\mathbf{r}d\mathbf{R}=rRdrdRd\phi_r d\phi_R=\tfrac{3}{2}\xi^3 d\xi d\beta d\phi_r d\phi_R. \quad (13)$$

We thus can define the density function associated with the size of the system

$$\rho(\xi)=\sum_i \int |F_{L\lambda i}|^2 \frac{3}{2}\xi^3 d\beta d\phi_r d\phi_R \quad (14)$$

fulfilling

$$\int \rho(\xi)d\xi=1. \quad (15)$$

Instead of using ϕ_r and ϕ_R, we use $\theta=\phi_r-\phi_R$ and ϕ_R as arguments, where θ is the angle between $\mathbf{r}$ and $\mathbf{R}$. Then we define the correlated density function associated with deformation

$$\rho(\theta,\beta)=\sum_i \int |F_{L\lambda i}|^2 \frac{3}{2}\xi^3 d\xi d\phi_R \quad (16)$$

fulfilling

$$\int \rho(\theta,\beta)d\theta d\beta=1. \quad (17)$$

We shall see that the feature of geometric structure and internal motion can be well understood via the above density functions. Obviously, for the one-dimensional representation $\lambda=\{3\}$ or $\lambda=\{1,1,1\}$, the summation over i in Eqs. (14) and (16) is not necessary.

V. PARTICLE CORRELATION

Let us make use of the density functions to extract information on particle correlation. We would like to clarify the following points.

(i) As a quantum-mechanic system, the character of the system depends decisively on how the wave function is distributed in coordinate space. In the case of spin-0 system, the distribution has been found to depend strongly on the accessibility of regular shapes [28], this is true, in particular, for the first states. For the present system of spin 1, let us investigate $\rho(\theta,\beta)$ of the first states with $L=0$ to 3 . Since the symmetry $\{3\}$ is just the symmetry of spin-0 systems, which has already been discussed in Ref. [28], we shall concentrate on the $\{2,1\}$ and $\{111\}$ symmetry, the associated $\rho(\theta,\beta)$ are plotted in Fig. 2.

It is noted that $\beta=0$, 1/4, 1/2, 3/4, and 1 correspond to $R/r=0$, 1/2, $\sqrt{3}/2$, 3/2, and ∞, respectively. Thus, in the θ-β plane, the point $(\theta,\beta)=(\pi/2,1/2)$ is associated with an ET, the points (0, 3/4) and $(\theta,0)$ are both associated with a CG1, the points (0, 1/4) and $(\theta,1)$ are both associated with another cigar shape with two particles located at the same end while the other one at the opposite end (denoted as CG2). With this in mind let us observe the contour diagrams of $\rho(\theta,\beta)$. Figures 2(b), 2(c), and 2(h) belong to type I, they are similar with each other, all peaked at the ET and spread to the CG1. Hence, just as the $0_1^{\{3\}}$ state of the spin-0 system [28], they are a mixture of the ET and the CG1, but the former is more important due to being lower in potential energy. Figure 2(e) belongs to type II, there is a peak at the ET, the distribution does not extend to the CG1. Figures 2(a), 2(d), and 2(f) belong to type III, they are similar, there is a peak at the CG1 but a well at the ET and a well at the CG2, thus they are mainly a collinear structure. Figure 2(g) belongs to type IV, there are no peaks at the ET nor at the CG1. The most probable distribution is associated with irregular triangles. Thus, these figures demonstrate clearly that, just as

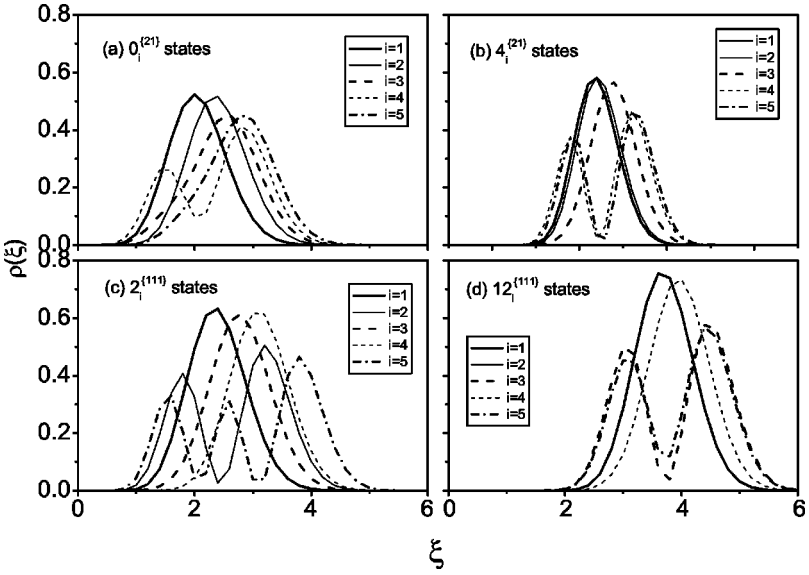

FIG. 3. $\rho(\xi)$ of the selected L_i^{λ} states. The thick solid line is for the $i=1$ state (the first state), the thin solid line for $i=2$, the thick dashed line for $i=3$, the thin dashed line for $i=4$, and the dashed-dotted line for $i=5$. The densities of 12_1^{111} and 12_2^{111} in Fig. 3(d) are almost same.

in the case of spin-0 systems [28], the structures of the first states depend decisively on their types or on their ability to get access to regular shapes. States having different L and λ would have similar structure if they belong to the same type.

It is emphasized that, if the interparticle interaction is not negligible, the total potential energy depends on the shape. Thus the accessibility of shapes affects not only the structures of wave function, but also the eigenenergies as discussed in Sec. III. Therefore, when the interaction is not weak, the analysis of the accessibility is an important step to understand the spectra.

(ii) Let us go beyond the first states and look at the modes of excitation. A detailed discussion on this subject has been given in Ref. [28]. Here, we shall focus on the breathing mode predicted by Pitaevskii and Rosch [27] based on the systems with zero-range interaction. For this purpose, $\rho(\xi)$ of selected states with {2,1} and {111} symmetry are given in Fig. 3. It was shown in Fig. 3(a) that $\rho(\xi)$ of the $0_4^{\{2,1\}}$ state has two peaks and a well, it implies that the oscillation associated with the variation of ξ, namely, the variation of the size, contains a node. In other words, the breathing mode has been excited. The calculated energy difference between $0_4^{\{2,1\}}$ and $0_1^{\{2,1\}}$ turns out to be 2.03, very close to the value of 2 for the excitation of the breathing mode given in Ref. [27]. The $\rho(\theta,\beta)$ diagram of $0_4^{\{2,1\}}$ is given in Fig. 4(a), which is nearly the same as Fig. 2(a). These facts implies that the $0_4^{\{2,1\}}$ and $0_1^{\{2,1\}}$ states have nearly the same internal structures, except their sizes. They belong to the same breathing band. Thus the Pitaevskii-Rosch oscillation predicted based on the zero-range interaction was found not only in the systems with the symmetry {3}, but also in the systems with other symmetries.

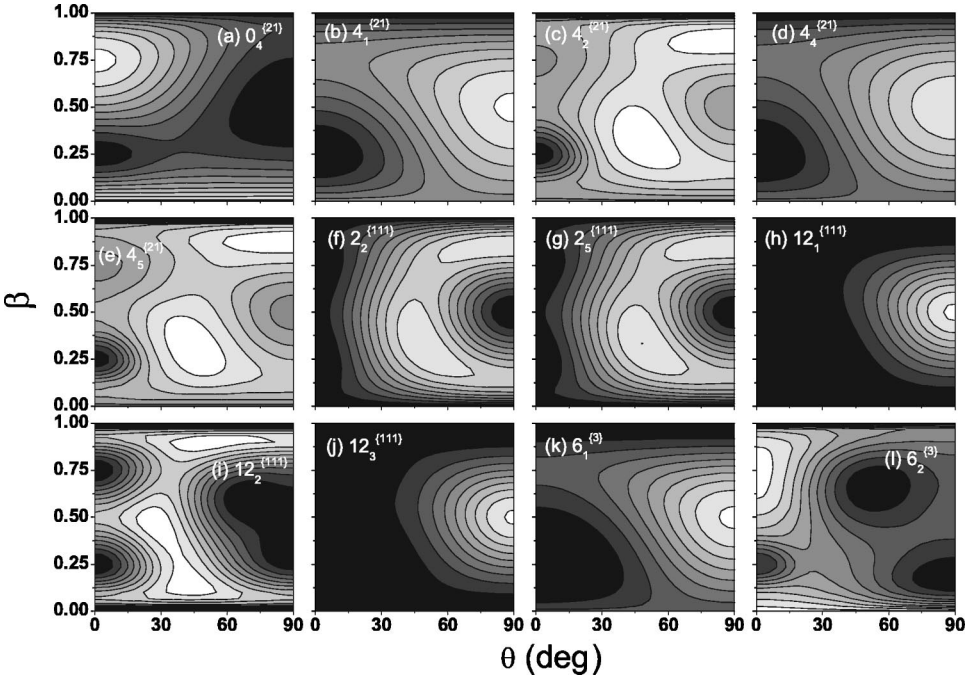

FIG. 4. $\rho(\theta,\beta)$ of selected $L_i^{\{2,1\}}$ and $L_i^{\{111\}}$ states.

Similarly, in Fig. 3(b) both the curves for the $4_4^{\{2,1\}}$ and $4_5^{\{2,1\}}$ states have two peaks. The calculated energy difference of the $4_4^{\{2,1\}}$ and $4_1^{\{2,1\}}$ states turns out to be 2.001, their $\rho(\theta,\beta)$ are very similar to each other as shown in Figs. 4(b) and 4(d). The energy difference of the $4_5^{\{2,1\}}$ and $4_2^{\{2,1\}}$ states turns out to be 2.009, their $\rho(\theta,\beta)$ are also very similar as shown in Figs. 4(c) and 4(e). Thus, the existence of the Pitaevskii-Rosch oscillation in $\lambda=\{2,1\}$ states is further confirmed.

In Fig. 3(c) the curve for $2_2^{\{111\}}$ has two peaks while the curve for $2_5^{\{111\}}$ has three peaks. $\rho(\theta,\beta)$ of these two states are shown in Fig. 4(f) and 4(g), they are very similar with each other and are more or less similar to that of the $2_1^{\{111\}}$ state shown in Fig. 2(g). The calculated energy of the $2_1^{\{111\}}$, $2_2^{\{111\}}$, and $2_5^{\{111\}}$ states turns out to be 6.005, 8.007, and 10.008, respectively, the separations are very close to 2. Thus the breathing band found in the spin-0 system [28] emerges again.

Examples for the states with a larger L are shown in Fig. 3(d), where both $12_3^{\{111\}}$ and $12_5^{\{111\}}$ have two peaks. $12_1^{\{111\}}$ and $12_3^{\{111\}}$ are the members of a breathing band, the similarity of their $\rho(\theta,\beta)$ is shown in Figs. 4(h) and 4(j), they are both peaked at an ET. $12_2^{\{111\}}$ and $12_5^{\{111\}}$ are the members of another higher breathing band, $\rho(\theta,\beta)$ of this band is shown in Fig. 4(i), where the wells originate from the nodal structure of wave function.

(iii) It has been mentioned earlier that, if two or more favorable basis functions with $k=K=0$ are contained in a L_i^λ series, the first state would be nearly free from the hard-core repulsion. Now, let us see how this happens. For an example, the $6_i^{\{3\}}$ series contains two favorable basis functions (cf. Table I). On the other hand, this series belongs to the type I (cf. Table III). Thus, it is expected that the first-state $6_1^{\{3\}}$ would have the same structure as $0_1^{\{3\}}$, $1_1^{\{21\}}$, and $2_1^{\{21\}}$, all of them belongs to the type I. Comparing Fig. 4(k) with Fig. 1(a) of Ref. [28], or with Figs. 2(b) and 2(c) of this paper, one can see that the θ-β diagram of $6_1^{\{3\}}$ is more concentrated surrounding the ET at $(\theta,\beta)=((\pi/2),1/2)$. Furthermore, it is recalled that the overlapping of two bosons is associated with the points $(0,\frac{1}{4})$ or $(\theta,1)$. The density function of $6_1^{\{3\}}$ shown in Fig. 4(k) keeps itself farther away from the above points, it implies that the two favorable basis functions have been coherently mixed up in such a way that the hard-core repulsion has been minimized. On the other hand, since the second state has to be orthogonal to the first state, $6_2^{\{3\}}$ has a completely different structure as shown in Fig. 4(l).

VI. ROTATING SYSTEMS

Recently, rotating Bose-Einstein condensates have been studied by some authors [19,21,22]. This is a very interesting subject because the rotation plays a role close to the role played by the magnetic field in quantum dots. Thus, the bosonic condensates and the electronic quantum dots have some features in common, e.g., the existence of magic angular momenta. Let the system be rotating with a uniform angular velocity Ω. We are interested in the lowest states when Ω is given. However, these lowest states might have the c.m. motion excited. Therefore, we shall take the c.m. motion into account in this section. For a given Ω, the series of eigenenergies reads $E^\lambda_{\Omega,j}=E^\lambda_{0,j}-(\Omega/\omega_0)\mathbf{L}$, where $E^\lambda_{0,j}$ is the energy of the system (including the energy of the c.m. motion) if $\Omega=0$, and $\mathbf{L}$ is the total orbital angular momentum (including the contribution from the c.m. motion). When Ω and λ are given, $E^\lambda_{\Omega,1}$ is the energy of the lowest state disregarding $\mathbf{L}$. These energies as a function of Ω are plotted in Fig. 5. It was found that $\mathbf{L}$ and λ of the ground state would jump if Ω varies. When Ω/ω_0 is changed from 0 to 1, $(\mathbf{L},\lambda)$ would jump from $(0,\{3\})$ to $(1,\{2,1\})$, $(2,\{2,1\})$, and $(3,\{111\})$. The transition of λ is a noticeable feature of the systems with nonzero spins.

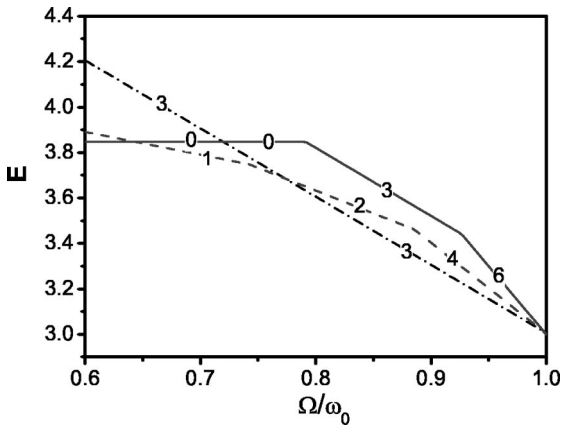

FIG. 5. $E^\lambda_{\Omega,1}$ as a function of Ω/ω_0. A piece of straight line is associated with the energy of a state with a given set of $\mathbf{L}$ and λ. $\mathbf{L}$ is marked at the line. The state with $\lambda=\{3\}$ is marked by a solid line, $\{2,1\}$ by a dashed line, and $\{111\}$ by a dashed-dotted line.

VII. EFFECT OF THE DETAILS OF INTERACTION

In the above calculation, the parameters $U=200$ and $b=0.1$ have been adopted. To see the effect of the details of interaction, two more cases are considered. One is a hard-core interaction with a longer range ($U=20$ and $b=0.316$), the other one is a zero-range interaction $\eta\delta(\mathbf{r}_i-\mathbf{r}_j)$ with $\eta=6.8$. The magnitudes of the new parameters are so chosen that the eigenenergies of the $0_1^{\{3\}}$ states in the above three cases are close to each other. The calculated results are given in Fig. 6, where the internal eigenenergies $E_i^{L,\{3\}}$ ($L=0-8$, $i=1,2$) are plotted. The three curves for the first states are very similar, those for the second states are also similar. Besides, the qualitative features of the associated density functions are also similar. Thus the qualitative features in the above three cases are similar. This fact implies that once the interaction remains to be repulsive and short range, the details of interaction does not seriously affect the feature of the system.

VIII. SUMMARY

We have presented numerical results of the low-lying states of an interacting two-dimension three-boson system

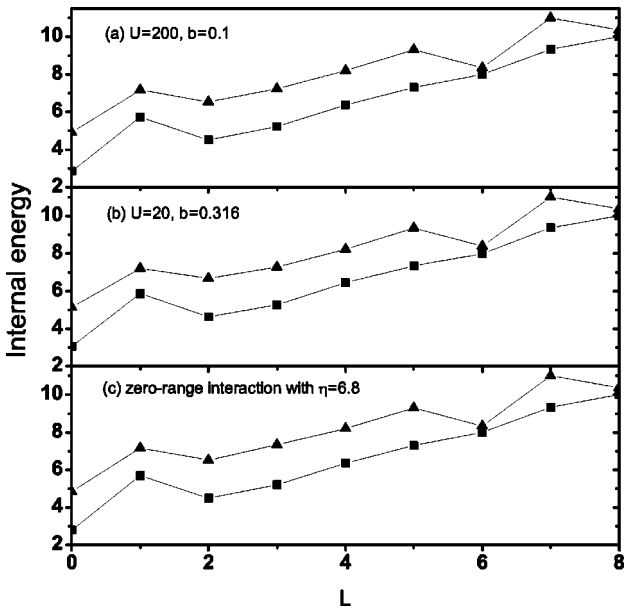

FIG. 6. $E_i^{L,\{3\}}$ ($i=1$ and 2, marked by a square and a triangle, respectively) with three kinds of interaction. (a) Repulsive hard-core with $U=200$ and $b=0.1$, (b) repulsive hard core with $U=20$ and $b=0.316$, (c) zero-range interaction with $\eta=6.8$.

with spin 1 and with hard-core interaction. The following points are noticeable.

(i) The densities functions $\rho(\theta,\beta)$ and $\rho(\xi)$ together can demonstrate very clearly the structures of states. When only the first states are concerned, there are only four kinds of θ-β diagram (cf. Figure 2) associated with four types of states (cf. Table III). The details of interaction affects the system only slightly (cf. Figure 6), if the repulsion remains to be of short range. This leads to a conclusion that the inherent nodal structure of wave functions plays a decisive role. The states with different L and λ might have similar structures, or even the states belonging to different bosonic systems (spin 0 or spin 1) might have similar structures if they belong to the same type, i.e., they have the same inherent nodal surfaces. Thus the analysis of the inherent nodal structures is a clue to understand these few-body systems.

(ii) When higher states are taken into account, the breathing mode of oscillation is important. This mode was first found by Pitaevskii and Rosch [27] in the bosonic systems with spin 0 and with zero-range interaction. However, in this paper, this mode is also found in our bosonic systems with spin 1 and with hard-core interaction. Due to the oscillation, the bands of breathing are formed. The members of the band can be well defined, they have nearly the same θ-β diagram but have distinct numbers of peak in $\rho(\xi)$.

In addition to breathing, the oscillation associated with the deformation of triangle is also found [cf. Figure 4(c)]. The two kinds of oscillations, breathing and deformation, can be excited simultaneously [cf. Fig. 4(e) and 3(b) for the $4_5^{\{21\}}$ state].

(iii) It is interesting to see that some states in the spectrum can avoid the hard-core repulsion nearly completely (e.g., $6_1^{\{3\}}$ has an energy 8.0000) via a coherent mixing of basis functions so that the distribution of the wave function can avoid the domain where overlap of particles occurs.

(iv) For rotating bosonic systems, the magic angular momenta and their transitions in a spin-1 system are very different from a spin-0 system, this is due to the transition of λ (cf. Fig. 5).

ACKNOWLEDGMENTS

This work was supported by the NSFC of China under Grant Nos. 90103028 and 10174098, and by a fund from the Ministry of Education.

[1] F. Dalfovo, S. Giorgini, L.P. Pitaevskii, and S. Stringari, Rev. Mod. Phys. **71**, 463 (1999).
[2] A.J. Leggert, Rev. Mod. Phys. **73**, 307 (2001).
[3] S. Stringari, Phys. Rev. A **58**, 2385 (1998).
[4] T.L. Ho and M. Ma, J. Low Temp. Phys. **115**, 61 (1999).
[5] A. Gorlitz *et al.*, Phys. Rev. Lett. **87**, 130402 (2001).
[6] C. Orzel *et al.*, Science **291**, 2386 (2001).
[7] F. Schreck *et al.*, Phys. Rev. Lett. **87**, 080403 (2001).
[8] M. Greiner *et al.*, e-print cond-mat/0105105.
[9] F. Zambelli and S. Stringari, Phys. Rev. Lett. **81**, 1754 (1998).
[10] A. Aftalion and T. Riviere, Phys. Rev. A **64**, 043611 (2001).
[11] A. Aftalion and Q. Du, Phys. Rev. A **64**, 063603 (2001).
[12] B. Mottelson, Phys. Rev. Lett. **83**, 2695 (1999).
[13] G.F. Bertsch and T. Papenbrock, Phys. Rev. Lett. **83**, 5412 (1999).
[14] G.M. Kavoulakis, B. Mottelson, and C.J. Pethick, Phys. Rev. A **62**, 063605 (2000).
[15] W.-J. Huang, Phys. Rev. A **63**, 015602 (2000).
[16] B. Paredes, P. Fedichev, J.I. Cirac, and P. Zoller, e-print cond-mat/0103251.
[17] G.M. Kavoulakis, B. Mottelson, and S.M. Reimann, Phys. Rev. A **63**, 055602 (2001).
[18] T. Papenbrock and G.F. Bertsch, Phys. Rev. A **63**, 023616 (2001).
[19] A.D. Jackson, G.M. Kavoulakis, B. Mottelson, and S.M. Reimann, Phys. Rev. Lett. **86**, 945 (2001).
[20] T. Nakajima and M. Ueda, Phys. Rev. A **63**, 043610 (2001).
[21] N.R. Cooper and N.K. Wilkin, Phys. Rev. B **60**, R16 279 (1999).
[22] N.K. Wilkin, J.M.F. Gunn, and R.A. Smith, Phys. Rev. Lett. **80**, 2265 (1998).
[23] R.A. Smith and N.K. Wilkin, Phys. Rev. A **62**, 061602(R) (2000).
[24] M. Manninen, S. Viefers, M. Koskinen, and S.M. Reimann, Phys. Rev. B **64**, 245322 (2001).
[25] M.A.H. Ahsan and N. Kumar, Phys. Rev. A **64**, 013608 (2001).
[26] X.J. Liu *et al.*, Phys. Rev. A **64**, 035601 (2001).
[27] L.P. Pitaevskii and A. Rosch, Phys. Rev. A **55**, R853 (1997).
[28] C.G. Bao *et al.*, Phys. Rev. A **65**, 022508 (2002).
[29] F. Chevy, V. Bretin, P. Rosenbusch, K.W. Madison, and J. Dali-

bard, Phys. Rev. Lett. **88**, 250402 (2002).
[30] M. Greiner, O. Mandel, T. Esslinger, T. Hansch, and I. Bloch, Nature (London) **415**, 39 (2002).
[31] M. Koashi and M. Ueda, Phys. Rev. Lett. **84**, 1066 (2000).
[32] T.-L. Ho and L. Yin, Phys. Rev. Lett. **84**, 2302 (2000).
[33] T.-L. Ho and E.J. Mueller, Phys. Rev. Lett. **89**, 050401 (2002).
[34] F. Zhou, Phys. Rev. Lett. **87**, 080401 (2001).
[35] J.W. Reijnders *et al.*, Phys. Rev. Lett. **89**, 120401 (2002).
[36] D.E. Rutherford, *Substitutional Analysis* (Edinburgh University Press, Edinburgh, 1948).
[37] C.G. Bao, Few-Body Syst. **13**, 41 (1992).
[38] Y.Z. He and C.G. Bao, J. Phys. B **34**, 1641 (2001).
[39] C.G. Bao, W.F. Xie, and W.Y. Ruan, Few-Body Syst. **22**, 135 (1997).